Microchimica Acta (2020) 187:574
https://doi.org/10.1007/s00604-020-04511-4

ORIGINAL PAPER

An electrochemical DNA biosensor based on nitrogen-doped graphene nanosheets decorated with gold nanoparticles for genetically modified maize detection

Fuli Liu[1] · Kai Li[2] · Yukun Zhang[1] · Jiaqi Ding[1] · Tingting Wen[1] · Xinwu Pei[3] · Yongliang Yan[3] · Wei Ji[1] · Jian Liu[1] · Xiao Zhang[1] · Liang Li[3]

Received: 21 May 2020 / Accepted: 18 August 2020

Abstract

A reliable electrochemical biosensor is reported based on nitrogen-doped graphene nanosheets and gold nanoparticle (Au/N-G) nanocomposites for the event-specific detection of GM maize MIR162. The differential pulse voltammetry response of methylene blue (MB) was chosen to monitor the target DNA hybridization event. Under the optimum conditions, the peak current increased linearly with the logarithm of the concentration of DNA in the range 1.0×10^{-14} to 1.0×10^{-8} M, and the detection limit was 2.52×10^{-15} M ($S/N = 3$). It is also demonstrated that the DNA biosensor has high selectivity, good stability, and fabrication reproducibility. The biosensor has been effectively applied to detect MIR162 in real samples, showing its potential as an effective tool for GM crop analysis. These results will contribute to the development of new portable transgenic detection systems.

Keywords Genetically modified crops · Electrochemical biosensor · Nitrogen-doped graphene · Gold nanoparticles · Portable detection

Introduction

According to the report of the International Service for the Acquisition of Agri-biotech Applications (ISAAA), 191.7 million hectares of biotech crops were grown in 26 countries worldwide in 2018, increasing ~113-fold from 1996 [1]. MIR162 is an insect-resistant GM maize event developed by Syngenta that contains a single copy of the modified vip3A gene and a mannose-6-phosphate isomerase (pmi) gene [2, 3]. In October 2013, the Shenzhen Port of China detected MIR162 GM maize that was not approved by the Ministry of Agriculture in a shipment of maize imported from the USA. As of February 2014, the amount of GM maize returned from China has exceeded 1.25 million tons, which has attracted widespread societal attention, and has obtained 43 approvals in 23 countries + EU 28 (counted as one). However, there is only one qualitative polymerase chain reaction (PCR) method for the detection of this event in China, and it is still necessary to develop a variety of detection methods.

Many analytical methods have been developed for accurate detection and quantification of GMOs and to verify compliance with legislation. PCR is the most common method. Quantitative real-time PCR (qPCR) is not only the gold standard for the quantitative analysis of GMO [4] but also the choice for detecting event-specific transgenes [5]. However, although PCR and qPCR are powerful and accurate, there are unavoidable shortcomings, such as complicated steps and not suitable for on-site analysis [6]. DNA biosensor has the advantages of simple operation, sensitivity, low cost, and easy automated analysis, and has been proposed as a new GMO

Electronic supplementary material The online version of this article (https://doi.org/10.1007/s00604-020-04511-4) contains supplementary material, which is available to authorized users.

✉ Jian Liu
756014310@qq.com

✉ Xiao Zhang
zhangxiao@cust.edu.cn

✉ Liang Li
liliang@caas.cn

[1] School of Life Science and Technology, Changchun University of Science and Technology, Changchun 130000, People's Republic of China

[2] College of Food Science and Nutritional Engineering, China Agricultural University, Beijing 100083, People's Republic of China

[3] Biotechnology Research Institute, Chinese Academy of Agricultural Sciences, Beijing 100081, China

Published online: 22 September 2020

analysis technology. Among the various types of DNA sensors, electrochemical sensors are among the earliest and most mature technologies because electrochemical reactions directly generate electrical signals and do not require expensive signal transduction equipment, resulting in the advantages of low cost, simple structure, and portability [7].

Recently, the use of nanomaterials to improve the sensitivity and specificity of electrochemical DNA biosensors has attracted great interest [8–10]. Due to their large surface area, superior conductivity [11], good biological compatibility [12], and low cost, graphene-based materials have been widely applied in constructing DNA sensors [13–15]. Studies show that the chemical activity, electronic properties, and optical properties of graphene can be tailored by adding appropriate dopants [16]. The most widely studied example is nitrogen-doped graphene (N-G). Compared with graphene, N-G has a larger functional surface area [17] and higher electrocatalytic activity [18, 19] and electrical conductivity [20, 21] so it is more widely used in supercapacitors, field effect transistors, and electrocatalysis. Its more chemically active sites than reduced graphene oxide (rGO) are also beneficial to the functionalization of metal nanoparticles [22].

Gold nanoparticles (AuNPs) are extensively used in DNA biosensors due to their high surface-to-volume ratio, good biocompatibility, and abilities to make the orientation of DNA more conducive to direct electron transfer and to easily link DNA through Au-S chemical bonds [23–26]. There have been some successful attempts to use N-G and AuNPs as composites in the electrochemical biosensor field [27]. Borowiec et al. [28] established a chloramphenicol sensor based on nitrogen-doped graphene nanosheets decorated with gold nanoparticles (Au/N-G) without using any redox mediators, indicating that Au/NG has a better electron transfer rate. Yang et al. [29] developed an electrochemical immunosensor for the detection of matrix metalloproteinase-2 using Au/N-G as an antibody-immobilized substrate and polydopamine-functionalized graphene oxide hybrid conjugated to horseradish peroxidase-secondary antibodies as a multi-labeled probe. Chen et al. also constructed an electrochemical sensor for human multidrug resistance genes using Au/N-G composites [30]. The use of N-G greatly increased the surface area and conductivity of the electrodes, while AuNPs further enhanced the fixation and hybridization capabilities of the probe DNA.

Here, we developed an electrochemical DNA biosensor constructed by AuNPs and an N-G nanomaterial–modified glassy carbon electrode (GCE) for GM MIR162 event-specific sequence detection. The principle is shown in Fig. 1. The hybridization event was detected through the MB redox signal by differential pulse voltammetry (DPV). Compared with the bare electrode, the modified Au/NG nanocomposite significantly improved the sensitivity of the biosensor because of the synergistic effect of AuNPs and N-G. As far as we know, there has been no previous related research.

Experimental

Chemicals and materials

Graphene oxide (GO) was ordered from Nanjing Jicang NanoTechnology Co., Ltd. Chloroauric acid ($HAuCl_4$) was purchased from Sangon (Shanghai, China). 6-Mercapto-1-hexanol (MCH) was supplied by Sigma-Aldrich (Shanghai, China). Methylene blue (MB) was provided by Solarbio (Beijing Solarbio Science & Technology Co., Ltd.). The MIR162 referential transgenic was kindly provided by the Chinese Academy of Agricultural Sciences, and non-transgenic maize samples were purchased from a local market. All of the synthetic oligonucleotide sequences and primers were ordered from Comate Bioscience Co., Ltd., and their sequences are listed in Table 1. All oligonucleotide stock solutions were prepared at a concentration of 10 μM in TE buffer solution (10 mM Tris-HCl, 1 mM EDTA, pH 8.0) and stored at − 20 °C in a refrigerator. Ultrapure water was used throughout this experiment.

Apparatus

Cyclic voltammetry (CV) and differential pulse voltammetry (DPV) were performed on a DH7001 electrochemical workstation. Ultrapure water was produced using a MicroPure (Thermo Scientific). Scanning electron microscope (SEM) images were recorded on a FEI Quanta 250 FEG (Thermo Scientific). XPS measurements were conducted using an ESCALAB 250 (Thermo Scientific). The phase composition of the samples was studied by X-ray diffraction (XRD) on a Bruker D8 Advance X-ray diffractometer with Cu Kα radiation. A BOX EF 2 gel imaging system was used for gel images.

Preparation of N-G and Au/N-G nanocomposites

See electronic supplementary material.

Biomodification of the sensor surface

The GCE surface was wet-polished to a mirror-like surface with an aqueous slurry of alumina powder, ultrasonicated with ethanol and water. Then, 5 μL of a 2.0 mg/mL Au/N-G suspension, which was prepared by dispersing Au/N-G powder in DMF, was coated on the electrode surface to obtain the Au/N-G/GCE and dried in air at room temperature. The rGO-modified GCE and the N-G-modified GCE were prepared in the same way. The thiol-functionalized capture probe (CP)

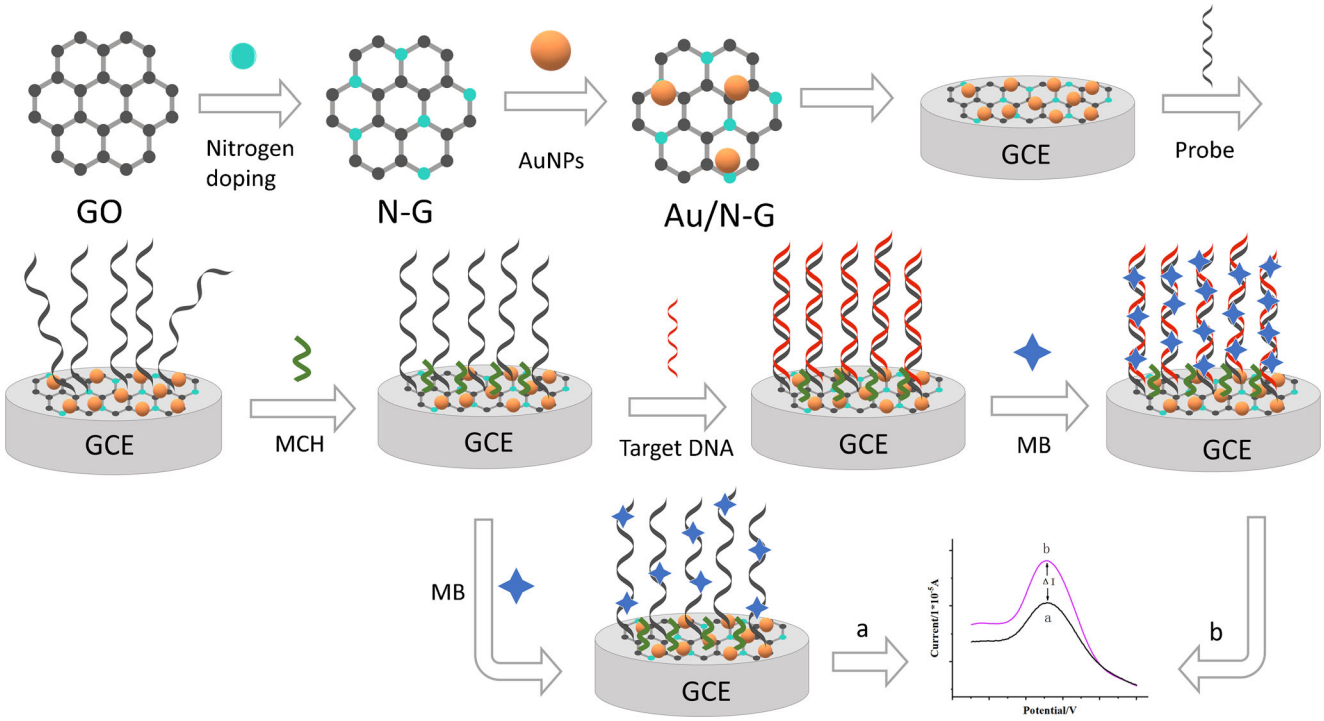

Fig. 1 Schematic illustration of the biosensor fabrication and detection procedures

was covalently anchored on the surface of the Au/N-G modified electrode by the thiol-Au interaction. Briefly, 5 μL of 10 μM ssDNA solution was drop-cast to cover the modified electrode and incubated for 1.5 h at room temperature. Then, the self-assembled electrode was washed with water to remove excess CP and incubated with 20 μL of 1 mM MCH at room temperature for 1 h to block nonspecific binding sites.

DNA extraction and PCR

A total of 0.1 g corn samples were ground into EP tubes and genomic DNA was extracted by CTAB-based method. The following thermal program was used: 94 °C for 5 min; 35 cycles of 94 °C for 30 s, 58 °C for 30 s, and 72 °C for 30 s; and a final extension at 72 °C for 3 min. PCR products were stored in a freezer. Amplicons (10 μL) were electrophoresed (100 V, 30 min) on a TB agarose gel (2%), stained with EB, and observed under ultraviolet light.

Hybridization with target DNA and electrochemical measurements

Hybridization was carried out by immersing CP/N-G/Au/GCE into 0.1 M PBS (pH 7.4) containing different concentrations of target DNA at 35 °C for 1 h. After hybridization, the DNA-modified electrode was washed with PBS to remove nonhybridized nucleic acids. MB accumulated on the modified electrode by immersing the modified electrode into 20 μM MB aqueous solution (containing 20 mM NaCl) for 20 min. Then, the electrode was washed with ultrapure water, washed in a stirred blank PBS buffer without MB for 5 min, and rinsed again with ultrapure water to remove any unbound

Table 1 The sequences of the oligonucleotides used in this study

Oligonucleotides	Sequences (from 5′ to 3′)
Capture probe	SH-GTCCGCCATGGTCTGAAGGCAACAG
Complementary sequences	CTGTTGCCTTCAGACCATGGCGGAC
One-base mismatch sequences	CTGTTGCCTTCAGAC**G**ATGGCGGAC
Two-base mismatch sequences	CTGTTGC**G**TTCAGAC**G**ATGGCGGAC
Noncomplementary sequences	ATCAAAAGGACCTGACTGCTCGCAA
PCR primer 1	GCGGTGTCATCTATGTTAC
PCR primer 2	GCCCAGTATGCCTTATCT

MB molecules. The electrochemical response was determined by DPV.

In the CV experiments, the desired modified electrode was immersed in 5 mM $[Fe(CN)_6]^{3-/4-}$ (with 0.1 M KCl) at a scan rate of 50 mV/s from − 0.2 to 0.6 V vs saturated calomel electrode (SCE). The DPV measurement conditions were as follows: amplitude: 25 mV, pulse width: 0.05 s, step width: 0.5 s, step height: 10 mV, scanning range: − 0.7 V to 0 V (vs. SCE), the current peak appears around − 0.35 V. To investigate the real sample hybridization, the process was as follows: DNA fragments after amplification were diluted 10 times with TE buffer (pH 7.4). The PCR-amplified samples were first thermally denatured at 95 °C for 5 min and then frozen on ice for 2 min. Then, the hybridization procedure was processed as before.

Results and discussion

Characterization of the N-G and Au/N-G nanocomposites

The morphologies of N-G and Au/N-G were characterized by SEM and TEM (see Fig. 2). N-G had a typical flake-like shape, and wrinkles could be seen on the surfaces, indicating that a high surface/volume ratio and two-dimensional structure were maintained. The wrinkle of N-G and its huge surface area can significantly expand the surface area of the working electrode, and is more conducive to loading gold nanoparticles. After AuNPs were reduced by EG, it can be seen that AuNPs were successfully reduced and evenly dispersed on the surface of N-G without agglomeration. Such a distribution is beneficial to increase the electrical conductivity of the composite and increasing the loading of probe DNA (Fig. 2B). The morphologies of N-G and Au/N-G were further confirmed by TEM characterization (Fig. 2C–D). The average diameter of AuNPs was estimated to be approximately 70 nm.

To further determine the surface chemical compositions and status of the N-G and Au/N-G, XPS analysis was conducted. As shown in Fig. 3B, the atomic ratio of O to C in N-G was calculated to be 14.6%, which was lower than that in GO of 47.1% because of the reduction reaction. On the other hand, the N 1s peak appears at approximately 400 eV compared with GO (Fig. 3A), indicating the successful doping of N in graphene. The atomic ratios of N to C in N-G and Au/N-G were calculated to be 11.1% and 7.5%, respectively. The different N/C atomic ratios were due to the influence of deposited Au on N-G. High-resolution N 1s spectra of these samples are shown in Fig. 3D. The N 1s spectrum could be clearly deconvoluted into three individual peaks, and the peaks at 398.9 eV, 400.1 eV, and 401.5 eV were attributed to pyridinic N, pyrrolic N, and graphite N configurations, respectively. Moreover, Au 4f peaks were observed at binding energies of 84 and 87 eV, corresponding to the binding energy of Au $4f_{7/2}$ and Au $4f_{5/2}$, respectively (Fig. 3E).

Moreover, the crystalline nature of GO, N-G, and Au/N-G was investigated by XRD (Fig. 3F). The GO (Fig. 3F, curve a) had a sharp peak at 11.7°. In N-G (Fig. 3F, curve b), this peak completely disappears, while a very broad peak at 24° is assigned to the hexagonal graphite structure C (0 0 2), indicating the recovery of the graphitic crystal structure. After gold loading, additional obvious peaks were observed at 38.3° (1 1 1), 44.5° (2 0 0), 64.7° (2 2 0), 77.6° (3 1 1), and 81.8° (2 2 2) (Fig. 3F, curve c), which are in good agreement with the reference pattern for cubic Au (JCPD 89-3697).

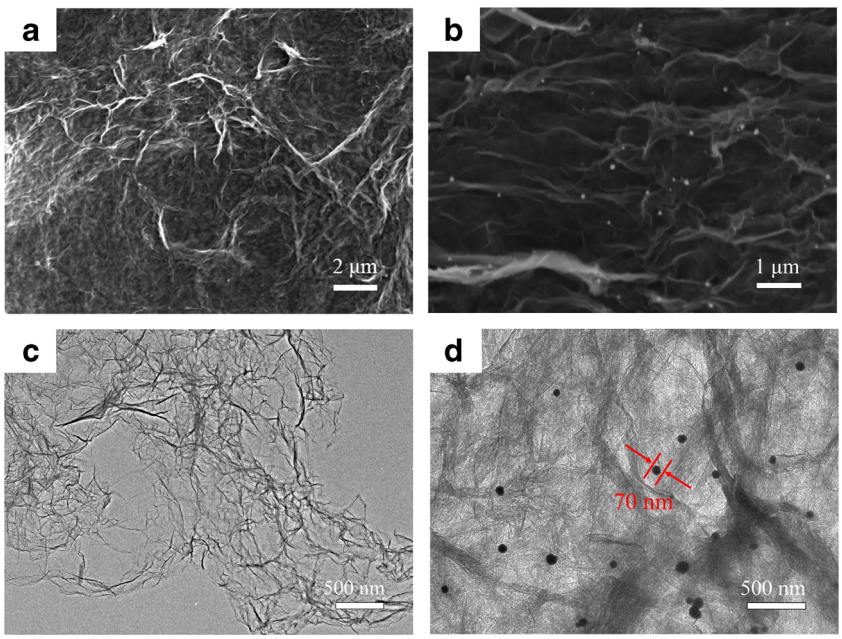

Fig. 2 SEM images of (A) N-G and (B) Au/N-G. TEM images of (C) N-G and (D) Au/N-G

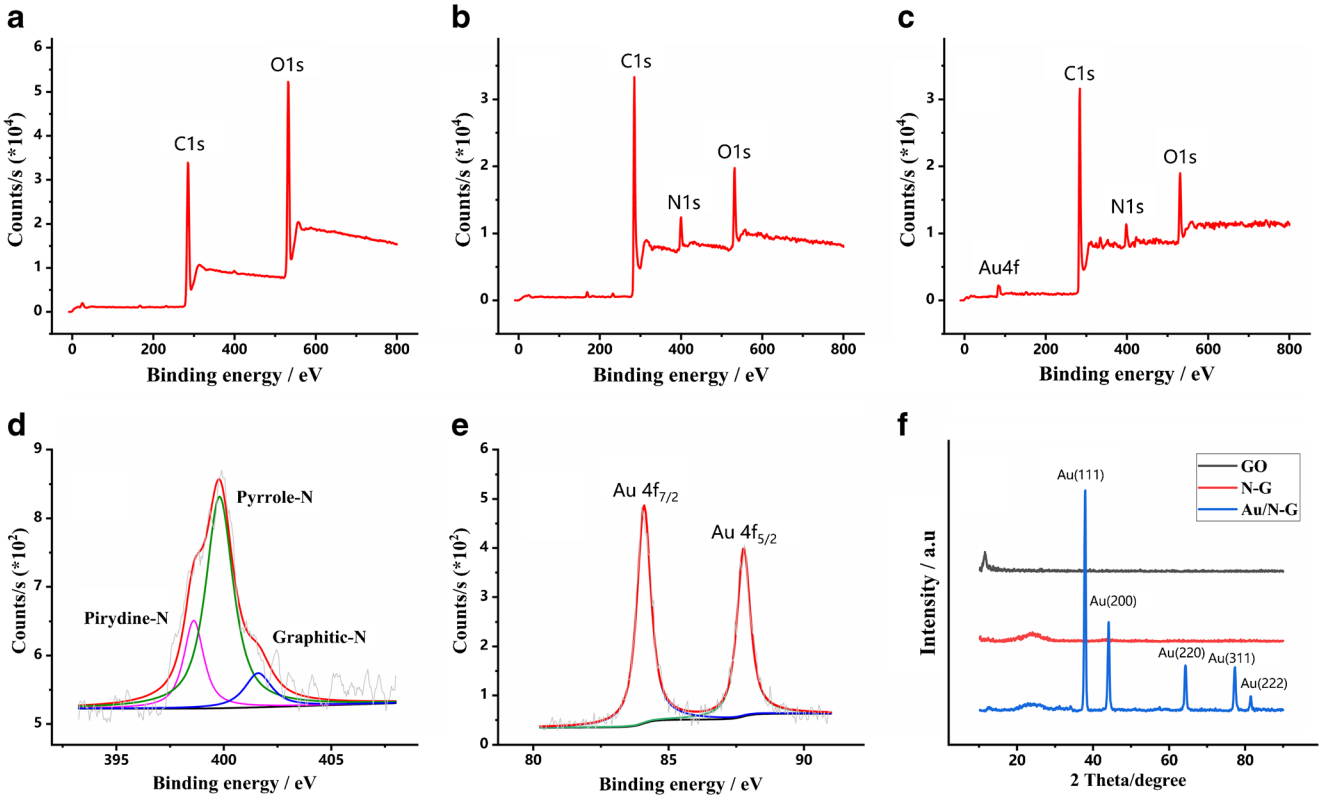

Fig. 3 XPS spectra of (A) GO; (B) N-G; (C) Au/N-G. High-resolution XPS spectrum of (D) N 1s and (E) Au 4f; (F) XRD patterns of GO (gray), N-G(red), Au/N-G(blue)

Electrochemical characterization

CV was applied to investigate the electrochemical performance of electrodes modified with different materials, and the experiment was carried out in a 5.0 mM $[Fe(CN)_6]^{3-/4-}$ solution (containing 0.1 M KCl). As shown in Fig. 4, it is clear that when rGO is assembled on the surface of GCE, the peak current (purple curve) obtained is much higher than the bare GCE (black curve), which can be attributed to the good conductivity of rGO. After assembling the N-G nanocomposite, the peak current (red curve) increased significantly compared with rGO, indicating that it has better conductivity. This is because the doping of N atoms causes more defect edges and surface defect points to appear on the N-G flakes, increasing the specific surface area and increasing the electron transfer rate. When the Au/N-G nanocomposite was assembled on the electrode surface, the highest peak current (blue curve) was obtained, indicating that the attachment of AuNPs significantly increased the electron transfer rate of the composite, which can be attributed to the excellent conductivity of AuNPs And the synergistic effect between N-G and AuNPs.

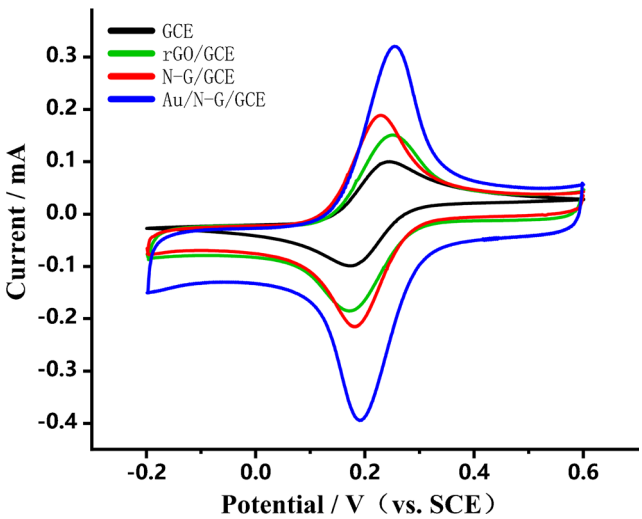

Fig. 4 Cyclic voltammograms of differentially modified electrodes in 5.0 mM Fe $(CN)_6^{3-/4-}$ solution (containing 0.1 M KCl) at a scan rate of 50 mV/s. Bare GCE (black); rGO/GCE (green); N-G/GCE (red); Au/N-G /GCE (blue)

Optimization of assay conditions

See electronic supplementary material.

Analytical performance of the DNA biosensor

The analytical performance of the fabricated DNA sensor was evaluated under the optimal conditions. The sensitivity of the DNA biosensor was evaluated by using various concentrations of target DNA for hybridization, and the experimental

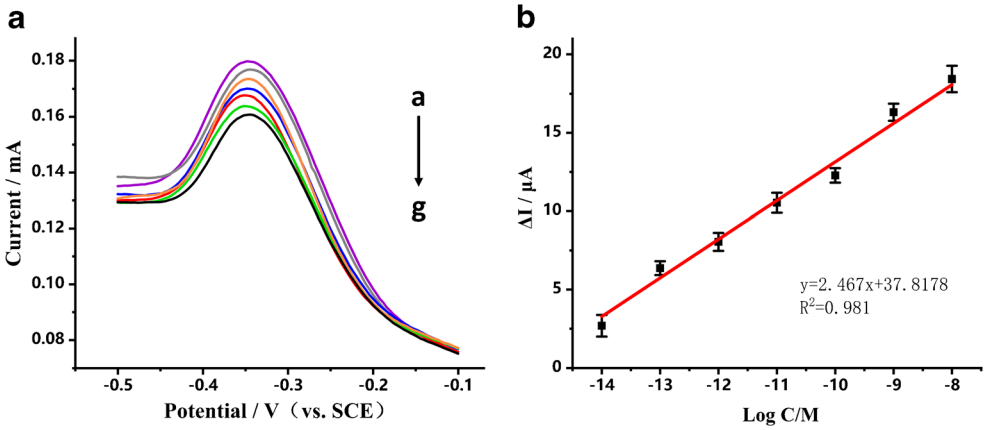

Fig. 5 The sensitivity test and standard curve of electrochemical DNA biosensor. (A) DPVs of MB accumulated on the hybridized ssDNA/Au/N-G/GCE with different concentrations of target DNA (1.0×10^{-8} M, 1.0×10^{-9} M, 1.0×10^{-10} M, 1.0×10^{-11} M, 1.0×10^{-12} M, 1.0×10^{-13} M, and 1.0×10^{-14} M curves a–g, respectively). (B) Relation of peak current versus log of concentration of target DNA. Amplitude: 25 mV, pulse width: 0.05 s, step width: 0.5 s, step height: 10 mV, scanning range: − 0.7 V to 0 V (vs. SCE), the current peak appears around − 0.35 V

results are shown in Fig. 5A. As presented, the peak current increased with increasing target DNA concentration. Figure 5 B shows a good linear relationship between the increase in peak currents and the logarithm of target DNA concentrations from 1.0×10^{-8} to 1.0×10^{-14} M. The linear regression equation was $\Delta I = 2.467x + 37.818$ with a correlation coefficient of 0.981. The detection limit was calculated to be 2.52×10^{-15} M ($S/N = 3$). Table 2 compares aspects of the analytical performance obtained in this research with that of other electrochemical DNA biosensors. We could see that the biosensor prepared in our work showed a broader linear range of DNA concentration and a lower detection limit.

The selectivity of the biosensor was evaluated by investigating the hybridization between ssDNA/Au/N-G/GCE with different mismatched sequences. The values of the corresponding peak current are shown as a histogram in Fig. S2. Compared with blank (blank data were shown in Table S2), the peak current of the noncomplementary sequence, two-base mismatch target, and one-base mismatch target gradually increase with decreasing mismatch degree. However, the increase is small. When ssDNA/Au/N-G/GCE hybridized with the complementary sequence, there was an obvious increase in the current. The peak current intensity was approximately 2.5 times that of the one-base mismatch. These DPV responses proved that the prepared DNA biosensor had good selectivity.

Reproducibility and stability of the biosensor

The fabrication reproducibility and stability were also investigated by detecting the target DNA at 1.0×10^{-8} M with five different ssDNA/Au/N-G/GCEs (Table S1). The relative standard deviation on the first day was calculated to be 5.7%, and there were no obvious response changes for each electrode after 1 week of refrigeration at 4 °C. These results indicated that the biosensor had high fabrication reproducibility and stability.

Detection in maize samples

The purpose of the prepared DNA biosensor was to determine the real maize sample. Therefore, to verify the practicality and detection effect of the biosensor, we mixed the same concentration of MIR162-positive maize and MIR162-negative

Table 2 Comparison of linear ranges and detection limits of the different electrochemical DNA sensors

Modified type	Detection method	Linear range (M)	Detection limit (M)	References
Au–PtNPs/Pty/GCE	EIS (label free)	1.0×10^{-12}–1.0×10^{-7}	3.6×10^{-13}	[31]
Gold nano urchin/rGO/SPCE	DPV with hematoxylin as indicator	1.0×10^{-13}–1.0×10^{-8}	3.5×10^{-14}	[32]
Au NRs-GO/GCE	DPV with MB as indicator	1.0×10^{-14}–1.0×10^{-9}	3.5×10^{-15}	[33]
p-RGO/CILE	DPV with MB as indicator	1.0×10^{-12}–1.0×10^{-6}	2.9×10^{-13}	[34]
nanoZrO_2/ERGO/GCE	DPV	1.0×10^{-13}–1.0×10^{-6}	2.0×10^{-15}	[35]
SWCNT/SPEs	DPV with ALP-Strp as substrate	2.5×10^{-10}–2.5×10^{-9}	6.4×10^{-11}	[36]
poly(nBA-NAS)/rGO/SPE	DPV with AQMS as indicator	1.0×10^{-15}–1.0×10^{-8}	6.3×10^{-16}	[37]
Au NPs/NG/GCE	DPV with MB as indicator	1.0×10^{-14}–1.0×10^{-8}	2.52×10^{-15}	This work

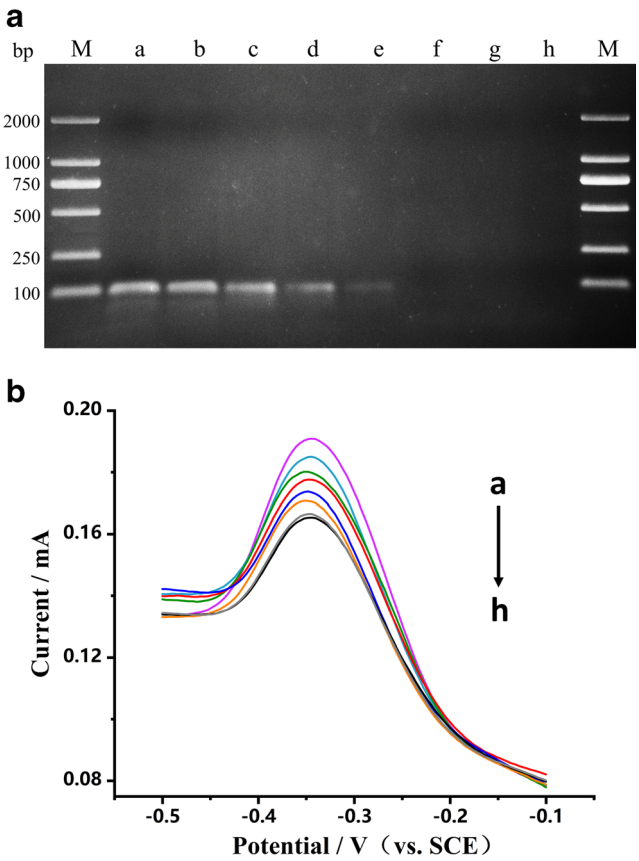

Fig. 6 Results of practical GMO sample detection. (A) Agarose gel electrophoresis and (B) DPV curves of different contents of MIR162 maize (m/m). M: DL2000 DNA marker. a–g: PCR products of mixed maize DNAs with 100%, 5%, 1%, 0.5%, 0.1%, 0.05%, and 0% MIR162 contents. h: no-template

maize genomic DNA into 7 samples in proportions of 100%, 5%, 1%, 0.5%, 0.1%, 0.05%, and 0% (w/w) MIR162. PCR products were then analyzed using agarose gel electrophoresis and biosensors. As shown in Fig. 6, the detection limit of MIR162 by PCR was 0.1%, but it could be clearly seen that the sensor method still had a higher current response to 0.05% of the sample. All the quantitative data of the real samples were shown in the Fig. S3. This could be attributed to the lower staining efficiency of EB, so that even if the product was successfully amplified by PCR, it was not visible on the agarose gel. These results indicated that the biosensor had good practicality, showing its good potential as a practical tool for MIR162 detection.

Conclusion

In this study, an electrochemical biosensor based on Au/N-G/GCE was reported for the detection of MIR162 maize. Due to the high surface/volume ratio and fast electronic transfer of the Au/N-G nanocomposite, the biosensor showed a wide detection range and low detection limit. In addition, it had good reproducibility and stability and could be used successfully for MIR162 sample analysis. All these data indicated that the designed DNA biosensor showed great potential in DNA analysis and could be integrated into a portable device to monitor the MIR162 event in the market, and can also be used to study other GMO organisms by simple modification of the probe, which is considered to have bright prospects in field analysis.

Funding information This work was supported by the National Natural Science Foundation of China (Grant No. 31200944), the National Key R&D Program of China (No. 2019YFA0904700), and the Agricultural Science and Technology Innovation Program of CAAS (no. CAAS-ZDRW202009).

Compliance with ethical standards

Conflict of interest The authors declare that they have no competing of interests.

References

1. James C (2019) Global status of commercialized biotech/GM crops in 2018. China Biotechnol 39:1–6
2. Long N, Bottoms J, Meghji MR, et al (2017) Corn Event MIR162
3. Takabatake R, Masubuchi T, Futo S et al (2014) Development and validation of an event-specific quantitative PCR method for genetically modified maize MIR162. Shokuhin Eiseigaku Zasshi 55:205–209
4. Marmiroli N, Maestri E, Gulli M et al (2008) Methods for detection of GMOs in food and feed. Anal Bioanal Chem 392:369–384
5. Fu W, Wang H, Wang C, Mei L, Lin X, Han X, Zhu S (2016) A high-throughput liquid bead array-based screening technology for Bt presence in GMO manipulation. Biosens Bioelectron 77:702–708
6. Manzanares-Palenzuela CL, Martín-Fernández B, Sánchez-Paniagua López M, López-Ruiz B (2015) Electrochemical genosensors as innovative tools for detection of genetically modified organisms. TrAC Trends Anal Chem 66:19–31
7. Sanchez-Paniagua Lopez M, Manzanares-Palenzuela CL, Lopez-Ruiz B (2018) Biosensors for GMO testing: nearly 25 years of research. Crit Rev Anal Chem 48:391–405
8. Xu K, Huang J, Ye Z, Ying Y, Li Y (2009) Recent development of nano-materials used in DNA biosensors. Sensors (Basel) 9:5534–5557
9. He S, Song B, Li D, Zhu C, Qi W, Wen Y, Wang L, Song S, Fang H, Fan C (2010) A craphene nanoprobe for rapid, sensitive, and multicolor fluorescent DNA analysis. Adv Funct Mater 20:453–459
10. Li L, Wen Y, Xu Q, Xu L, Liu D, Liu G, Huang Q (2015) Application of carbon nanomaterials in gene delivery for endogenous RNA interference in vitro and in vivo. Curr Pharm Des 21:3191–3198
11. Hu W, Peng C, Lv M, Li X, Zhang Y, Chen N, Fan C, Huang Q (2011) Protein corona-mediated mitigation of cytotoxicity of graphene oxide. ACS Nano 5:3693–3700
12. Chen H, Müller MB, Gilmore KJ, Wallace GG, Li D (2008) Mechanically strong, electrically conductive, and biocompatible graphene paper. Adv Mater 20:3557–3561

13. Pumera M (2009) Electrochemistry of graphene: new horizons for sensing and energy storage. Chem Rec 9:211–223
14. Pumera M, Ambrosi A, Bonanni A, Chng ELK, Poh HL (2010) Graphene for electrochemical sensing and biosensing. TrAC Trends Anal Chem 29:954–965
15. Cao X (2014) Ultra-sensitive electrochemical DNA biosensor based on signal amplification using gold nanoparticles modified with molybdenum disulfide, graphene and horseradish peroxidase. Microchim Acta 181:1133–1141
16. Giribabu K, Suresh R, Manigandan R, Praveen Kumar S, Muthamizh S, Munusamy S, Narayanan V (2014) Preparation of nitrogen-doped reduced graphene oxide and its use in a glassy carbon electrode for sensing 4-nitrophenol at nanomolar levels. Microchim Acta 181:1863–1870
17. Long D, Li W, Ling L, Miyawaki J, Mochida I, Yoon SH (2010) Preparation of nitrogen-doped graphene sheets by a combined chemical and hydrothermal reduction of graphene oxide. Langmuir 26:16096–16102
18. Chen P, Xiao TY, Qian YH, Li SS, Yu SH (2013) A nitrogen-doped graphene/carbon nanotube nanocomposite with synergistically enhanced electrochemical activity. Adv Mater 25:3192–3196
19. Liu X, Li Z, Ding R, Ren B, Li Y (2016) A nanocarbon paste electrode modified with nitrogen-doped graphene for square wave anodic stripping voltammetric determination of trace lead and cadmium. Microchim Acta 183:709–714
20. Lee SU, Belosludov RV, Mizuseki H, Kawazoe Y (2009) Designing nanogadgetry for nanoelectronic devices with nitrogen-doped capped carbon nanotubes. Small 5:1769–1775
21. Hassan M, Jiang Y, Bo X, Zhou M (2018) Sensitive nonenzymatic detection of hydrogen peroxide at nitrogen-doped graphene supported-CoFe nanoparticles. Talanta 188:339–348
22. Chen M, Hou C, Huo D, Fa H, Zhao Y, Shen C (2017) A sensitive electrochemical DNA biosensor based on three-dimensional nitrogen-doped graphene and Fe3O4 nanoparticles. Sensors Actuators B Chem 239:421–429
23. Cai H, Xu C, He P, Fang Y (2001) Colloid Au-enhanced DNA immobilization for the electrochemical detection of sequence-specific DNA. J Electroanal Chem 510:78–85
24. Liu S, Leech D, Ju H (2003) Application of colloidal gold in protein immobilization, electron transfer, and biosensing. Anal Lett 36:1–19
25. Yanez-Sedeno P, Pingarron JM (2010) Gold nanoparticle-based electrochemical biosensors. Anal Bioanal Chem 382:884–886
26. Fang X, Jiang W, Han X, Zhang Y (2013) Molecular beacon based biosensor for the sequence-specific detection of DNA using DNA-capped gold nanoparticles-streptavidin conjugates for signal amplification. Microchim Acta 180:1271–1277
27. Shekari Z, Zare HR, Falahati A (2019) Electrochemical sandwich aptasensor for the carcinoembryonic antigen using graphene quantum dots, gold nanoparticles and nitrogen doped graphene modified electrode and exploiting the peroxidase-mimicking activity of a G-quadruplex DNAzyme. Microchim Acta 186:530
28. Borowiec J, Wang R, Zhu L, Zhang J (2013) Synthesis of nitrogen-doped graphene nanosheets decorated with gold nanoparticles as an improved sensor for electrochemical determination of chloramphenicol. Electrochim Acta 99:138–144
29. Yang G, Li L, Rana RK, Zhu J-J (2013) Assembled gold nanoparticles on nitrogen-doped graphene for ultrasensitive electrochemical detection of matrix metalloproteinase-2. Carbon N Y 61:357–366
30. Chen M, Hou C, Huo D, Bao J, Fa H, Shen C (2016) An electrochemical DNA biosensor based on nitrogen-doped graphene/Au nanoparticles for human multidrug resistance gene detection. Biosens Bioelectron 85:684–691
31. Yang T, Zhou N, Li Q, Guan Q, Zhang W, Jiao K (2012) Highly sensitive electrochemical impedance sensing of PEP gene based on integrated Au–Pt alloy nanoparticles and polytyramine. Colloids Surfaces B Biointerfaces 97:150–154
32. Aghili Z, Nasirizadeh N, Divsalar A, Shoeibi S, Yaghmaei P (2017) A nanobiosensor composed of exfoliated graphene oxide and gold nano-urchins, for detection of GMO products. Biosens Bioelectron 95:72–80
33. Han X, Fang X, Shi A, Wang J, Zhang Y (2013) An electrochemical DNA biosensor based on gold nanorods decorated graphene oxide sheets for sensing platform. Anal Biochem 443:117–123
34. Sun W, Zhang Y, Hu A, Lu Y, Shi F, Lei B, Sun Z (2013) Electrochemical DNA biosensor based on partially reduced graphene oxide modified carbon ionic liquid electrode for the detection of transgenic soybean A2704-12 gene sequence. Electroanalysis 25:1417–1424
35. Xueliang W, Zhaoxia W, Tao W, Xiaohui DAI (2019) Electrochemical determination of the specific genetic sequence in transgenic maize using reduced graphene oxide and nano zirconia composites as a platform for immobilizing DNA. Chin J Appl Chem 36:839–846
36. Fortunati S, Rozzi A, Curti F, Giannetto M, Corradini R, Careri M (2019) Novel amperometric genosensor based on peptide nucleic acid (PNA) probes immobilized on carbon nanotubes-screen printed electrodes for the determination of trace levels of non-amplified DNA in genetically modified (GM) soy. Biosens Bioelectron 129:7–14
37. Jamaluddin RZAR, Heng LY, Tan LL, Chong KF (2018) A biosensor for genetic modified soybean DNA determination via adsorption of anthraquinone-2-sulphonic acid in reduced graphene oxide. Electroanalysis 30:250–258